Geomech. Geophys. Geo-energ. Geo-resour. (2020)6:38
https://doi.org/10.1007/s40948-020-00161-1

ORIGINAL ARTICLE

A new approach to evaluate the particle size distribution from rock drilling: double peak characteristic analysis

Xiaofeng Yang · Derek Elsworth · Jiaheng Zhou · Aiguo Nie · Liyuan Liu

Received: 9 January 2020 / Accepted: 22 April 2020

Abstract The characteristics of the particle size distribution (PSD) are an important reflection of energy consumption during rock drilling and drilling efficiency. A new approach incorporating both fine and coarse fractions of the PSD to supplement the typical approach of merely utilizing D50 (50% passing diameter) to index drilling resistance and efficiency is reported in this paper. A series of drilling experiments are conducted on limestone with variable rotation rate and with measured response of both penetration rate and PSD. The PSD organizes into a bimodal distribution with two distinct peaks corresponding to fine (Peak I) and coarse (Peak II) fractions. The mean size of Peak I is mainly conditioned by the rock property and the contact angle of the drilling tool. Peak II results from the effects of grinding and comminution and is conditioned by operational drilling parameters of rotation speed and the penetration rate of the bit. With an increase in bit penetration rate, the mean particle size of Peak II increases and its volume percentage decreases. With an increase in rotation rate, the mean particle size of Peak II initially decreases before slightly increasing at higher rates, while sympathetically, its volume percentage initially increases before decreasing. Such mechanistic analyses applied to define the resulting form of the PSD suggest operational changes that may be used to control the resulting PSD and optimize drilling.

Keywords Rock drilling · Particle size distribution · Size grade regions · Double peak characteristic · Formation mechanism

1 Introduction

Rock drilling is a key activity in the extraction of fluids from subsurface reservoirs, including water from aquifers, petroleum, natural gas and gas hydrate from hydrocarbon reservoirs and thermal fluids from geothermal reservoirs (Hood and Alehossein 2000; Ren et al. 2013; Kwon et al. 2014; Ma et al. 2016; Zhang and Zhao 2020). The drilling design and operation must consider the constraints related to both safety and economic considerations. Many previous experimental, numerical, and theoretical studies have been conducted to investigate drilling strategies in

X. Yang (✉) · J. Zhou · A. Nie
School of Mechanics and Civil Engineering, China University of Mining and Technology, Beijing 100083, China
e-mail: xfyang@cumtb.edu.cn

D. Elsworth
Department of Energy and Mineral Engineering, EMS Energy Institute and G3 Center, Pennsylvania State University, University Park, State College, PA 16801, USA

L. Liu
School of Civil and Resource Engineering, University of Science and Technology Beijing, Beijing 100083, China

Published online: 01 May 2020

terms of rock properties and to optimize the drilling parameters to achieve ultimate drilling efficiency. However, rock drilling is an intrinsically complex process involving mechanical kinetics, rock mechanics, material tribology, and fluid mechanics (Bondarenko et al. 2013; Lou et al. 2016; Che et al. 2016; Rahimi and Nygaard 2018). Even though significant improvements have been made in the fundamental understanding of rock drilling, critical unknowns influencing underlying mechanisms that affect drilling efficiency still remain (Thomas and Filippov 1999; Ciccu and Grosso 2013; Martins 2016; Wu and Han 2009; Che et al. 2012a, b).

The characteristics of the drilling comminution products are closely linked to drilling efficiency. The particle size distribution (PSD) directly reflects energy consumption during rock drilling process (Weichert 1991). Furthermore, the PSD can influence the performance of the drilling fluid which is related to both drilling resistance and efficiency (Peysson 2004). Generally, the smaller the average size of the resulting comminuted particles the greater the drilling energy consumed—due to the increase in surface area created (Vogt 2016; Zhao et al. 2015). The PSD also exerts a strong impact on the rheology of the drilling fluid, influencing the efficiency of removing the drilling products with a related feedback on drilling performance (Gamwo and Kabir 2015; Abrams 1977). The particles production of a uniform distribution of appropriate size within the drilling fluid would improve fluid rheology and reduce the consumption of drilling energy—but at the expense of increased energy consumption of comminution. The resulting PSD also affects the heat dissipation capacity of the drilling detritus with a potential feedback of increased wear and damage of the bit (Yang et al. 2014; Beste et al. 2001, 2006). There is an approximate correlation between the rate of advance and the size range of particles—the higher the rate of advance the larger the mean particle size (Pfleider and Blake 1953) with this also influenced by bit pressure, rate of advance, and bit-roughness (Miller 1986; Ersoy and Waller 1997). Thus, the understanding, prediction and control of the drilling-induced PSD are important and have significant effects on drilling efficiency and costs (Jimeno et al. 1995).

Although PSD is a key indicator of drilling efficiency and energy consumption, the current principal evaluating indicator remains as a single mean particle size diameter D50 (50% passing size). This neglects potential nuances in information contained within the full PSD which may provide important clues to mechanisms controlling drilling resistance and efficiency.

This study presents a new approach to analyze the particle size distribution resulting from rock drilling and to understand the contributing mechanisms. Laboratory drilling experiments are completed at variable rotation and penetration rate on limestone and the full PSD of the rock drilling particles are measured. These observations are used to define the main factors affecting PSD characteristics and their related mechanisms.

2 Materials and experimental methods

Dry drilling experiments are completed with the detrital products gathered and analyzed by laser classifier.

2.1 Materials

The sedimentary limestone specimens were collected from the Mentougou Mine to the west of Beijing and characterized for uniaxial compressive strength, direct shear strength, and thermal conductivity tests (Table 1).

2.2 Experimental procedure

The drilling experiments are conducted in a bench drilling system, as shown in Fig. 1. The blade of the auger bit is cemented carbide YG8 with a diameter of 7.94 mm.

The two experimental variables are the rotation rate, Z, and the penetration rate, T, with each parameter specified at 5 levels (Table 2). Full suite of drilling experiments is completed under each rotation and penetration rate.

These parameters are electronically controlled to obtain stable rates throughout the drilling operation. Each rotation rate is matched to 5 penetration rates, resulting in a total of 25 drilling tests, each 30 mm in depth (drilling length). The drilling detritus from each test is recovered and air-dried and comprises approximately 10 g for each sample (Fig. 2). PSDs of the drilling samples are measured in a Malvern

Table 1 Mechanical and thermal properties of limestone from the Mentougou Mine, Beijing

Compressive strength (MPa)	Shear strength (MPa)	Shear angle (°)	Density (10^3 kg/m^3)	Thermal conductivity (W/mk)
145.4	14.7	67	2.6	2.4

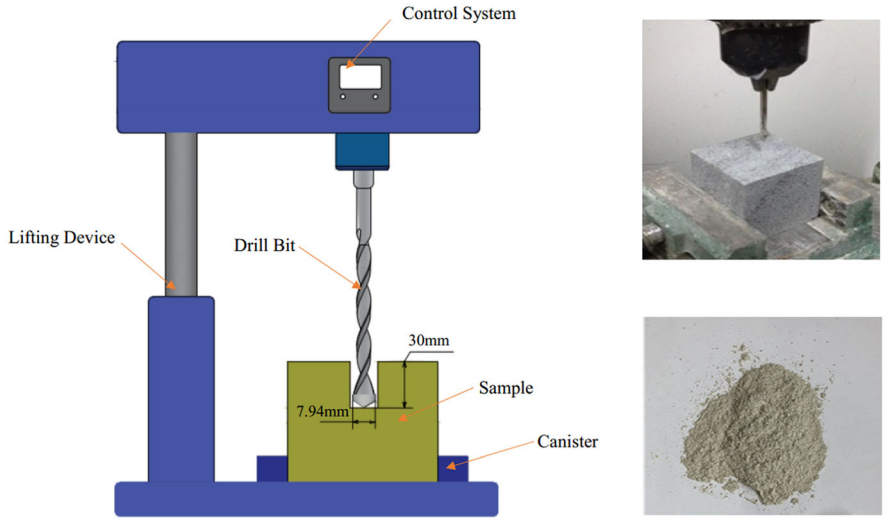

Fig. 1 Rock sample and drilling equipment

Table 2 Operational parameters for the drilling experiments

Rotation	Z1	Z2	Z3	Z4	Z5
(r/min)	600	900	1250	1750	2600
Penetration	T1	T2	T3	T4	T5
(mm/s)	0.75	0.85	1.0	1.2	1.5

with three repeat measurements completed for each of the 25 tests.

3 Results and discussion

We analyze the characteristics of the PSD from the drilling experiments. The PSD is classified over its full

Fig. 2 Morphology of the rock drilling particles

Mastersizer 3000 (Fig. 3), using laser diffraction to measure the PSD in the range 0.01 μm to 3.5 mm, range and used to define principal mechanisms contributing to rock breakage and penetration that

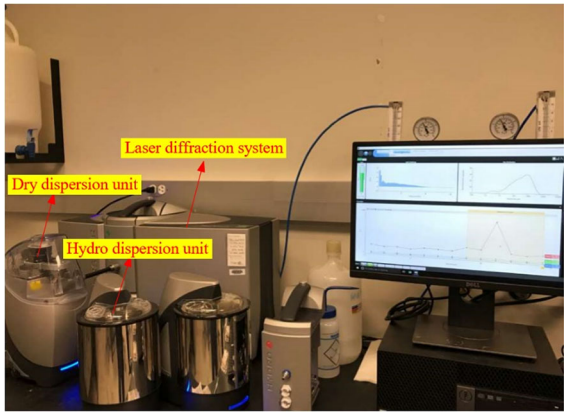

Fig. 3 Particle size distribution measurement system

are distributed between the two peaks of a bimodal distribution.

3.1 Integral analysis of PSD characteristics

Cumulative PSDs measured by the laser classifier are shown for all drilling samples in Fig. 4. Particle sizes are principally in the range 1–100 μm with little content either < 1 μm or > 100 μm. The distributions of the coefficient of nonuniformity Cu ($\mathrm{Cu} = \frac{D60}{D10}$), are plotted with the operational parameters in Fig. 4—drilling with a higher penetration or rotation rate increases the nonuniformity. However, at intermediate rotation rates, the Cu represents uniformity than at either high and low rotation rates. Furthermore, the PSD curve for a penetration rate of 1.0 mm/s and a rotation speed of 1750 revolutions per minute (rpm) results in a minimum D50 (22 μm), with a maximum D50 (42.1 μm) resulting for a penetration rate of 1.5 mm/s and rotation rate of 600 rpm.

The PSD curves (66 sampling points in each curve) for all the full suite of experiments are shown in Fig. 5. The drilling particle size can be classified into three primary categories: (1) fine particle fraction with sizes in the range 0.1–1 μm; (2) intermediate particles fraction (1–100 μm); and (3) coarse particle fraction (100–400 μm). Two clear peaks are apparent in each PSD curve as shown in Fig. 3. Peak I represents the fine fraction where the peak represents a particle diameter of 0.3 ± 0.04 μm and a volume percentage of $0.5 \pm 0.08\%$. Peak II represents the coarse fraction where the peak represents a particle diameter of 55–90 μm and a volume percentage of $3.3 \pm 0.2\%$. It should be noted that the particle size of Peak II is greater than D50. The PSD profile of the fine particle region remains near constant for all operational drilling parameters. In contrast, the intermediate and coarse particle fractions are broadly distributed with, and therefore highly sensitive to, the applied operational drilling parameters. This results in a distribution of peak particle sizes and significant variability in their relative volume (Fig. 5).

3.2 Mechanisms contributing to fines fraction (Peak I)

The form of the PSD is a direct result of rock breakage by drilling. The drilling process consists of successive cycles of penetration and rotation (Li and Itakura 2012). From an analytical standpoint, this process may be divided into two separate stages—drill bit penetration to a certain depth followed by rotation at this depth to shear off a cutting and leaving an empty kerf. When repeated, this results in helical penetration and a spiraled discharge of drill cuttings.

The penetrated rock is initially crushed by the concentrated stress applied beneath the drill bit. The rock fails when this stress exceeds the compressive strength of the rock (Fig. 6a) leaving the surrounding rock to be sheared by the rotation of the bit blade—when the cutting stress exceeds the shear strength. The comminution into particles occurs principally during the normal penetration, with this penetration contributing the main source of fine particles comprising the fine fraction (Peak I).

A dense core results when the rock is penetrated by the indenter (Chen and Labuz 2006) with this representing the main source of the finest particles. The size of this dense core defines the proportion of fine particles created during active drilling (Peak I). Based on the penetration model of Fig. 6a, the penetration volume is expressed as,

$$V_p = \frac{\pi h^3 tan^2 \frac{\theta}{2}}{3} \tag{1}$$

where θ is the top angle of the indenter; a is half of the projected contact length of the penetration, h is the penetration depth which is mainly related to the compressive properties of rock such as compressive strength and the friction and dilatancy angles (Huang 1999). Thus, the dense core volume V_d is given by

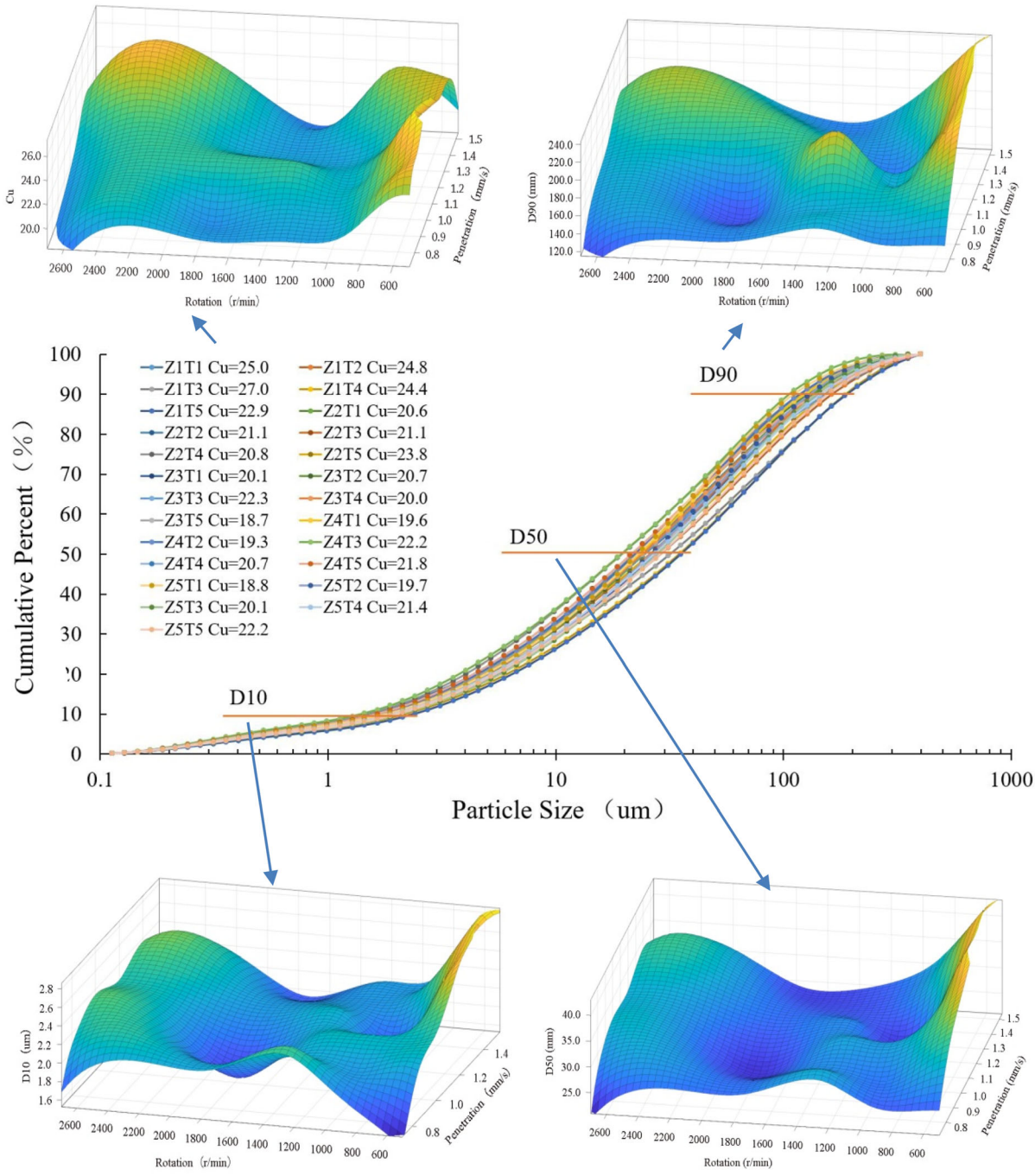

Fig. 4 Cumulative PSDs for different drilling operational conditions

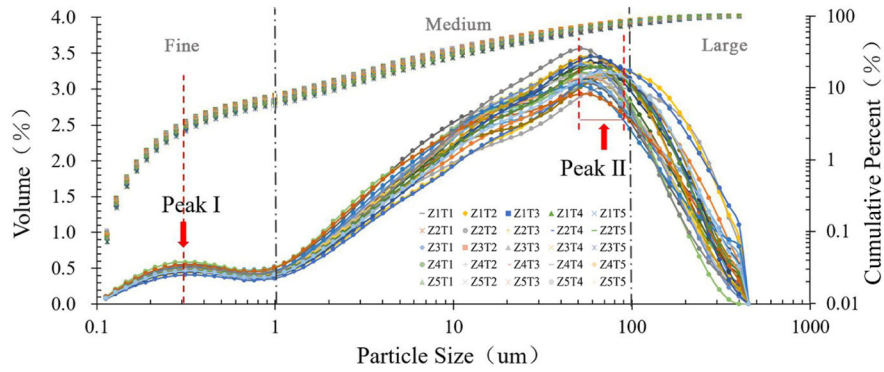

Fig. 5 Particle size distributions for different drilling operation conditions

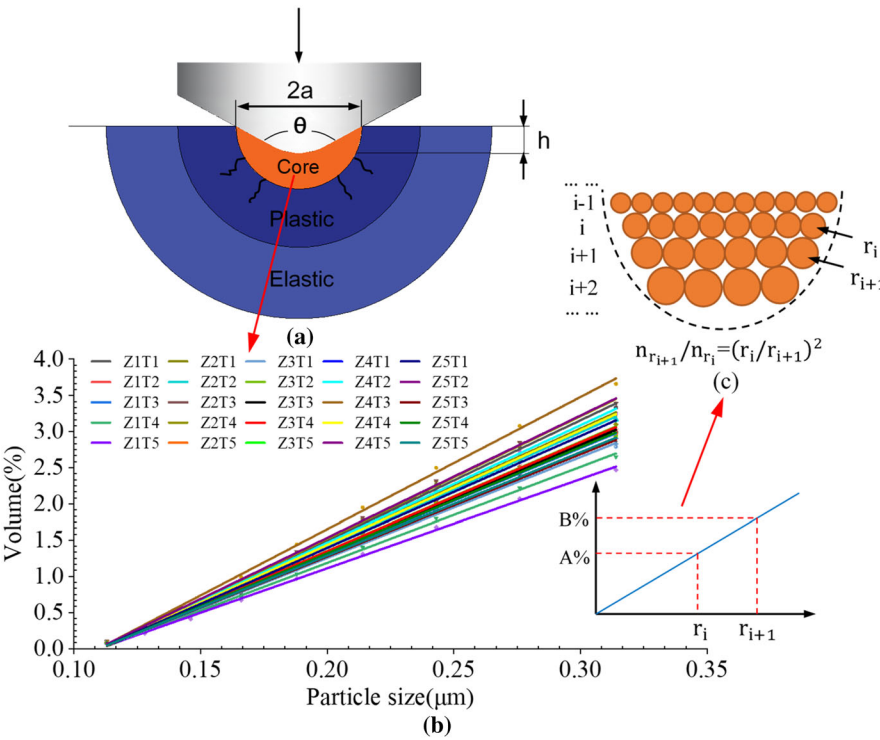

Fig. 6 Schematic of a rock penetration model

$$V_d = \frac{2\pi h^3 tan^3\frac{\theta}{2} - \pi h^3 tan^2\frac{\theta}{2}}{3} \quad (2)$$

and is controlled by the geometry of the drilling tool and rock properties. Thus, we can infer that the operational drilling parameters exert negligible influence on the size of the dense core, based on this theoretical description.

In addition, apparent from the experimental data, is that the cumulative distribution of particle sizes smaller than Peak I is near linear (Fig. 6b). Assuming the diameter of any single particle size on this straight line as r_i, the number of particles is n_{r_i} and the volume percentage is A%. Correspondingly, the diameter of any adjacent point is r_{i+1}, with a number of particles as $n_{r_{i+1}}$ and a percentage is B%. The diameter ratio between these two adjacent points is $\frac{r_{i+1}}{r_i}$, resulting in,

$$\frac{B}{A} = \frac{n_{r_{i+1}} \times \frac{4}{3} \times \pi \times (r_{i+1})^3}{n_{r_i} \times \frac{4}{3} \times \pi \times (r_i)^3}. \quad (3)$$

Accordingly, accepting the linearity of cumulative volume with particle diameter apparent in Fig. 6b, yields,

$$\frac{B}{r_{i+1}} = \frac{A}{r_i}. \tag{4}$$

Combining Eqs. (3) and (4), the ratio of the number of particles of two adjacent diameters comprising the dense core of fines (Peak I) may be simplified as

$$\frac{n_{r_{i+1}}}{n_{r_i}} = \left(\frac{r_i}{r_{i+1}}\right)^2. \tag{5}$$

This defines the ratio of the number of adjacent particles is inversely proportional to the square of their diameter ratio for the fine particles before Peak I (Fig. 6c).

3.3 Mechanisms contributing to coarse fraction (Peak II)

The coarse fraction (Peak II) is presumed to be created by bit rotation that immediately follows the bit penetration that created the initial fine fraction (Peak I) as a result of crushing. The fractured fragments, created by this bit rotation, are subsequently ground by the movement of the drill bit during the continuous drilling process. However, the initial PSD representing the coarse fraction (Peak II) is posited to result from this initial shearing, before a portion of this is ground finer by crushing. The experimental results (Figs. 7, 8) show that the position of the peak volume consist of the coarse fraction (Peak II) is significantly impacted by the bit penetration and rotation rates. The mean particle size represented by Peak II increases and volume fraction decreases as the bit penetration rate increases (Fig. 7). This suggests that the proportion of particles in the intermediate and coarse particle fractions increase with an increase in penetration rate. Note that, for the same length of drilling, the

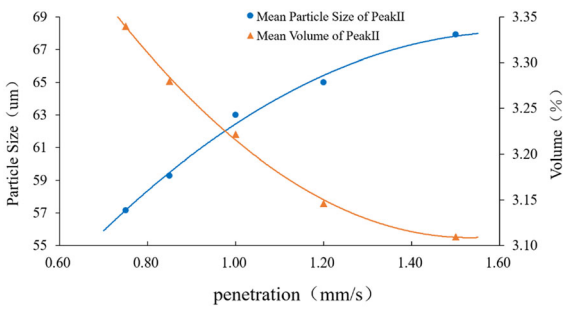

Fig. 7 Effect of penetration on the mean particle size distribution of the coarse fraction produced (Peak II)

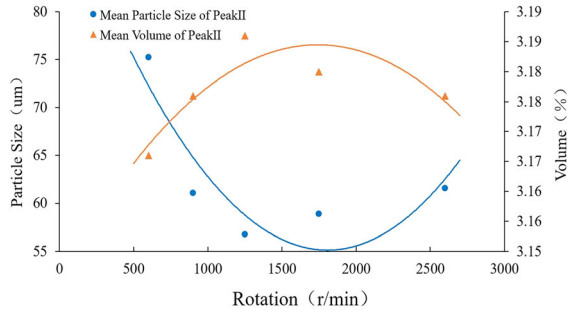

Fig. 8 Effect of rotation rate on the mean particle size distribution of the coarse fraction produced (Peak II)

comminution time will decrease as the penetration rate increases, thus the particle size will increase as a result of this shortened duration for comminution.

Rotation rate exerts a more complicated effect on the formation of the coarse fraction (Peak II). At lower rotation rates (< 1750 r/min), the mean particle size of Peak II decreases and the peak amplitude of volume percentage increases (Fig. 8) with an increase in rotation rate (for invariant penetration rate). Conversely however, for higher rotation rates (1750 r/min), the mean particle size of Peak II increases and the peak amplitude of volume percentage decreases (Fig. 8) with an increase in rotation rate (for invariant penetration rate). These results relate two mechanisms of particle grinding present in the process of bit rotation. The first is contact wear caused by the relative movement between adjacent particles, and the second represents impact wear between particles. Impact wear is more effective in grinding than contact wear when the particles are energetic and have high impact velocities (Tuomas et al. 2006). Grinding mainly results from contact wear between the adjacent particles at a lower bit rotation rates where particle velocities are correspondingly lower. As bit rotation rate increases, the particles rotate with the bit and drop from a certain height, induced by the impact wear between the particles, and thus the effects of particle grinding are reinforced. The higher the bit rotation speed, the higher position the particles will fall from. However, the particles will also rotate with the bit under centrifugal force rather than falling when the angular velocity of the bit is above a critical speed. In this situation, the effectiveness of grinding will significantly decrease enabling a greater number of the larger particles to survive and therefore increase the mean particle size of Peak II. Thus, in general, the

fraction of fines represented by Peak I is a reflection of rock properties, while Peak II is a reflection of drilling parameters. The combined evaluation of Peak I and Peak II could contribute to better comprehend particle characteristics and optimize the size distribution of rock drilling.

4 Conclusions

A new approach to analyze the particle size distribution resulting from rock drilling and to understand contributing mechanisms is presented. Laboratory rock drilling experiments and full PSD measurements are completed to define the main factors affecting PSD characteristics and their related mechanisms. The following conclusions are drawn:

1. Analyses of PSDs indicate that the particle size distribution is bimodal, classifying into two distinct peaks size fractions. The features of the fine particle fraction (Peak I) are negligibly affected by bit rotation speed rate or penetration speed, but instead are influenced by rock strength. Conversely, the features of the intermediate and especially the coarse fraction of generated particles (Peak II) are strongly influenced by operational drilling parameters.
2. Two mechanisms are explored to explain the bimodal form of the PSDs observed as a result of drilling. The formation of Peak I results from crushing beneath the bit and is determined by the contact angle of the bit and the rock property. The formation of Peak II results from the effects of grinding and comminution and is conditioned by the rotation speed and the penetration rate of the bit. With an increase in bit penetration rate, the mean particle size of Peak II increases and its volume percentage decreases. With an increase in rotation rate, the mean particle size of Peak II initially decreases before slightly increasing at higher rates, while sympathetically, its volume percentage initially increases before decreasing.
3. Clear from these experiments and analyses are that the fraction of fines (Peak I) is principally a reflection of rock and tool properties, while the coarse fraction (Peak II) is a reflection of operational parameters of rotation and penetration rates. Such mechanistic analyses applied to define the resulting form of the PSD suggest operational changes that may be used to control the resulting PSD and optimize drilling.

Acknowledgements This work is supported by National Natural Science Foundation of China (Nos. 51674122 and 51874310).

Compliance with ethical standards

Conflict of interest The authors declare that they have no conflicts of interest regarding the publication of this paper.

References

Abrams A (1977) Mud design to minimize rock impairment due to particle invasion. J Pet Technol 29:586–592. https://doi.org/10.2118/5713-pa

Beste U, Hartzell T, Engqvist H, Axén N (2001) Surface damage on cemented carbide rock-drill buttons. Wear 249:324–329. https://doi.org/10.1016/S0043-1648(01)00553-1

Beste U, Coronel E, Jacobson S (2006) Wear induced material modifications of cemented carbide rock drill buttons. Int J Refract Metal Hard Mater 24:168–176. https://doi.org/10.1016/j.ijrmhm.2005.05.003

Bondarenko P, Andreyev V, Savchuk V, Matviichuk O, Ievdokymova V, Galkov V (2013) Recent researches on the metal–ceramic composites based on the decamicron-grained WC. Int J Refract Metal Hard Mater 39:18–31. https://doi.org/10.1016/j.ijrmhm.2013.01.018

Che D, Han P, Guo P, Ehmann K (2012a) Issues in polycrystalline diamond compact cutter–rock Interaction from a metal machining point of view—part I: temperature, stresses, and forces. J Manuf Sci Eng. https://doi.org/10.1115/1.4007468

Che D, Han P, Guo P, Ehmann K (2012b) Issues in polycrystalline diamond compact cutter–rock Interaction from a metal machining point of view—part II: bit performance and rock cutting mechanics. J Manuf Sci Eng. https://doi.org/10.1115/1.4007623

Che D, Zhu W, Ehmann F (2016) Chipping and crushing mechanisms in orthogonal rock cutting. Int J Mech Sci 119:224–236. https://doi.org/10.1016/j.ijmecsci.2016.10.020

Chen L, Labuz F (2006) Indentation of rock by wedge-shaped tools. Int J Rock Mech Min Sci 4:1023–1033. https://doi.org/10.1016/j.ijrmms.2006.03.005

Ciccu R, Grosso B (2013) Improvement of disc cutter performance by water jet assistance. Rock Mech Rock Eng 47:733–744. https://doi.org/10.1007/s00603-013-0433-4

Ersoy A, Waller D (1997) Drilling detritus and the operating parameters of thermally stable PDC core bits. Int J Rock Mech Min Sci 34:1109–1123. https://doi.org/10.1016/s1365-1609(97)90203-3

Gamwo K, Kabir A (2015) Impact of drilling fluid rheology and wellbore pressure on rock cuttings removal performance:

numerical investigation. Asia-Pac J Chem Eng 10:809–822. https://doi.org/10.1002/apj.1917

Hood M, Alehossein H (2000) A development in rock cutting technology. Int J Rock Mech Min Sci 37:297–305. https://doi.org/10.1016/S1365-1609(99)00107-0

Huang H (1999) Discrete element modeling of rock-tool interaction. PhD thesis, University of Minnesota

Jimeno E, Jimeno C, Carcedo F (1995) Drilling and blasting of rocks. CRC Press, Boca Raton

Kwon K, Song C, Park J, Oh J, Lee J, Cho J (2014) Evaluation of drilling efficiency by percussion testing of a drill bit with new button arrangement. Int J Precis Eng Manuf 15:1063–1068. https://doi.org/10.1007/s12541-014-0437-3

Li Z, Itakura K (2012) An analytical drilling model of drag bits for evaluation of rock strength. Soils Found 52:216–227. https://doi.org/10.1016/j.sandf.2012.02.002

Lou L, Wu W, Liang X (2016) Analysis of the cutting features of the damaged rock by shock disturbance. Open Pet Eng J 9:159–168. https://doi.org/10.2174/1874834101609160159

Ma T, Chen P, Zhao J (2016) Overview on vertical and directional drilling technologies for the exploration and exploitation of deep petroleum resources. Geomech Geophys Geo-Energy Geo-Resour 2:365–395. https://doi.org/10.1007/s40948-016-0038-y

Martins S (2016) Size-energy relationship in comminution, incorporating scaling laws and heat. Int J Miner Process 153:29–43. https://doi.org/10.1016/j.minpro.2016.05.020

Miller D (1986) Rock drilling with impregnated diamond bits. PhD thesis, University of Cape Town, Cape Town, South Africa

Peysson Y (2004) Solid/liquid dispersions in drilling and production. Oil Gas Sci Technol-Revue D Ifp Energies Nouvelles 59:11–22. https://doi.org/10.2516/ogst:2004002

Pfleider E, Blake R (1953) Research on the cutting action of the diamond drill bit. Min Eng 5:187–195

Rahimi R, Nygaard R (2018) Effect of rock strength variation on the estimated borehole breakout using shear failure criteria. Geomech Geophys Geo-Energy Geo-Resour 4:369–382. https://doi.org/10.1007/s40948-018-0093-7

Ren X, Miao H, Peng Z (2013) A review of cemented carbides for rock drilling: an old but still tough challenge in geo-engineering. Int J Refract Metal Hard Mater 39:61–77. https://doi.org/10.1016/j.ijrmhm.2013.01.003

Thomas A, Filippov O (1999) Fractures, fractals and breakage energy of mineral particles. Int J Miner Process 57:285–301. https://doi.org/10.1016/S0301-7516(99)00029-0

Tuomas K, Pekka S, Päivi K, Jari L (2006) Impact wear in mineral crushing. Proc Est Acad Sci 12:408–418

Vogt D (2016) A review of rock cutting for underground mining: past, present, and future. J South Afr Inst Min Metall 116:1011–1026. https://doi.org/10.17159/2411-9717/2016/v116n11a3

Weichert R (1991) Theoretical prediction of energy-consumption and particle-size distribution in grinding and drilling of brittle materials. Part Part Syst Charact 8:55–62. https://doi.org/10.1002/ppsc.19910080111

Wu J, Han D (2009) A new approach to predicting the maximum temperature in dry drilling based on a finite element model. J Manuf Process 11:19–30. https://doi.org/10.1016/j.jmapro.2009.07.001

Yang X, Wu S, Kang Y, Wang X, Xia R (2014) Pitting mechanism of cemented carbide tool in the early stage of rock drilling. Int J Refract Metal Hard Mater 42:103–107. https://doi.org/10.1016/j.ijrmhm.2013.08.009

Zhang Y, Zhao G (2020) A global review of deep geothermal energy exploration: from a view of rock mechanics and engineering. Geomech Geophys Geo-Energy Geo-Resour 6:4. https://doi.org/10.1007/s40948-019-00126-z

Zhao X, Yao X, Gong Q, Ma H, Li X (2015) Comparison study on rock crack pattern under a single normal and inclined disc cutter by linear cutting experiments. Tunn Undergr Space Technol 50:479–489. https://doi.org/10.1016/j.tust.2015.09.002